Intense paramagnon excitations in a large family of high-temperature superconductors

M. Le Tacon, J. Chaloupka, M.W. Haverkort, V. Hinkov, S. Blanco-Canosa, M. Bakr, G. L. Sun, Y. T. Song, C. T. Lin, G. Khaliullin, and B. Keimer

The twenty-fifth anniversary of the discovery of high-temperature superconductivity is approaching without a compelling theory of the mechanism underlying this phenomenon. After the discovery of an unconventional (d-wave) symmetry of the Cooper pair wave function in the copper oxides, the thrust of research has been focused on the role of repulsive Coulomb interactions between conduction electrons, which naturally explain this pairing symmetry. However, since even simple models based on repulsive interactions have thus far defied a full solution, the question of whether such interactions alone can generate high-temperature superconductivity is still open. A complementary, more empirical approach has asked whether antiferromagnetic (AF) spin fluctuations can mediate Cooper pairing in analogy to the phonon-mediated pairing mechanism in conventional superconductors. This scenario requires the existence of well-defined AF spin fluctuations in the superconducting range of the cuprate phase diagram (for mobile hole concentrations $5\% \leq p \leq 25\%$ per copper atom), well outside the narrow stability range of AF long-range order ($0 \leq p \leq 2\%$). An extensive series of experiments using inelastic spin-flip scattering of neutrons has indeed revealed low-energy spin fluctuations in doped cuprates (see ref. 1 and refs. therein), but, for cuprate compounds hosting the most robust superconducting states (those that are optimally doped to exhibit $T_c \geq 90$ K), inelastic neutron scattering (INS) experiments have thus far mostly revealed spin excitations over a narrow range of excitation energies $E \sim 30 - 70$ meV, wave vectors $\mathbf{Q}$ covering only ~ 10 % of the Brillouin zone area around the AF ordering wave vector $\mathbf{Q}_{AF}$, and temperatures $T < T_c$. The energy- and momentum-integrated intensity of these excitations constitutes only a few percent of the spectral weight of spin waves in antiferromagnetically ordered cuprates, and is thus clearly insufficient to support high-$\mathrm{T_c}$ superconductivity. The apparent weakness of AF fluctuations in optimally doped compounds has been used as a central argument against magnetically mediated pairing scenarios for the cuprates. This picture is, however, strongly influenced by technical limitations of the INS method that arise from the small cross section of magnetic neutron scattering in combination with the weak primary flux of currently available high-energy neutron beams. Because of intensity constraints, even the detection of undamped spin waves in antiferromagnetically ordered cuprates over their full band width of ~ 300 meV has required samples with volumes of order 10 cm^3, which are very difficult to obtain. Doping further reduces the intensity of the INS profiles and exacerbates these difficulties.

Here we take advantage of recent progress in the development of high-resolution resonant inelastic x-ray scattering (RIXS) in order to explore magnetic excitations in a wide energy-momentum window that has been largely hidden from view by INS. Experiments on undoped cuprates have shown that RIXS with photon energies at the Cu L_3 absorption edge is sensitive to single-magnon excitations by virtue of the strong spin-orbit coupling of the $2p_{3/2}$ core-hole intermediate state, in excellent agreement with INS measurements. We have applied this method to the well characterized $YBa_2Cu_3O_{6+x}$ ($YBCO_{6+x}$) family. One of the great advantages of RIXS over INS is that it allows measurements of magnetic excitations with sizable intensity over much of the accessible reciprocal space, even on very small sample volumes. The results presented here have been obtained on thin films and on millimeter-sized single crystals far below the volume requirements of INS. Figure 1 shows a sketch of the scattering geometry of our experiment, as well as RIXS spectra obtained on undoped AF $NdBCO_6$ (Fig. 1 b,c) and underdoped superconducting $NdBCO_7$ (Fig. 1 d,e), for incident photon polarizations in and out of the scattering plane (π and σ geometries).

For undoped AF $NdBCO_6$, we can decompose the response in the mid-infrared (MIR) region of the spectra (Fig. 1c) for energy losses below ~ 500 meV following the method employed in Ref. 2. In the π scattering geometry, this leads to (i) an intense resolution-limited peak around 250 meV, (ii) a high-energy tail of this peak centered around 400 meV, and (iii) a weak low-energy contribution around 100 meV. In the σ scattering geometry, feature (i) is strongly suppressed, which allows us to assign this feature to a single-magnon excitation, in agreement with theoretical considerations and previous investigations on other cuprates (ref. 2). The weaker features (ii) and (iii) are associated with higher-order spin excitations and lattice vibrations, respectively. The energy of the single-magnon feature in $NdBCO_6$ depends strongly on the momentum transfer $Q_{//}$ as can be seen in Fig. 2a. Fitting our data using the spin-wave dispersion calculated for a bilayer in the framework of a simple Heisenberg model, we obtain $J_{//}$=133 $\pm$ 2 meV and $J_{\perp}$=12 $\pm$ 3 meV for the intra- and inter-layer exchange constants, respectively, in excellent agreement with previous INS data. We now turn to the doped systems, investigated here over a wide range of doping levels: strongly underdoped $NdBCO_7$ and $YBCO_{6.6}$ (T_c = 65 K and 61 K, respectively), weakly underdoped $YBa_2Cu_4O_8$ (T_c = 80 K), and weakly overdoped $YBCO_7$ (T_c = 90 K). Because of their stoichiometric composition and electronic homogeneity, the latter two compounds

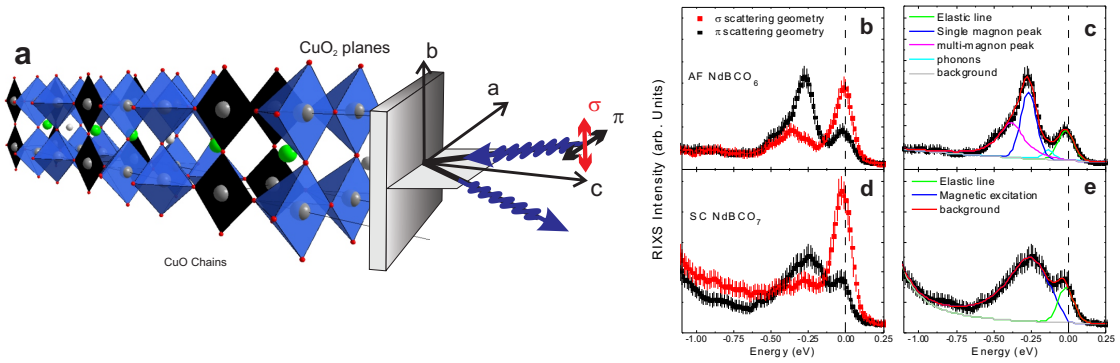

Figure 1: a) Schematics of the scattering geometry. Typical RIXS spectra of undoped AF $Nd_{1.2}Ba_{1.8}Cu_3O_6$ (b, c) and superconducting underdoped $Nd_{1.2}Ba_{1.8}Cu_3O_7$ (d,e), obtained at T = 15 K for $Q_{//}$=0.37 r.l.u., in both π (black squares) and σ (red squares) scattering geometries.

have served as model compounds in the experimental literature on high-T_c superconductivity, but apart from the "resonant mode" that appears in $YBCO_7$ below T_c no information has been available on their magnetic excitation spectra. The broad MIR features seen in Fig. 1d are present at all doping levels in the same energy range as the single-magnon peak in undoped $NdBCO_6$. They obey the same polarization dependence as the magnon mode (Figs. 1 e), and are therefore assigned to magnetic excitations. Based on the metallic nature of the doped cuprates, one expects strong damping of magnetic excitations in the Stoner continuum of incoherent electron-hole excitations. We have therefore fitted these spectra to Voigt profiles that are the result of the convolution of the Lorentzian lineshape of excitations with finite lifetime with the Gaussian resolution function. Since the fits yield excellent agreement with this simple profile (solid lines in Figs. 1 e), we can accurately extract the energies and half-widths-at-half-maximum (HWHM) of the magnetic excitation as a function of the transferred momentum (Fig. 3b,c).

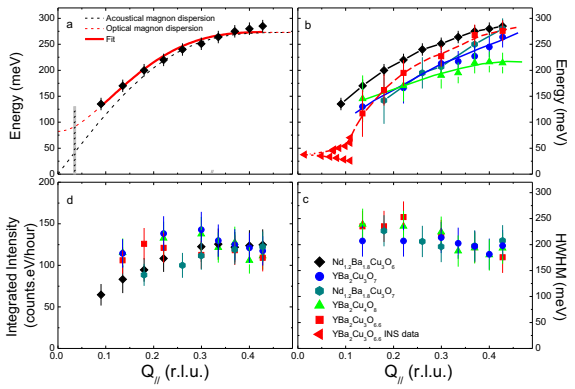

Figure 2: (a) Experimental magnon dispersion in AF $Nd_{1.2}Ba_{1.8}Cu_3O_6$, fitted using the spin-wave dispersion of a bilayer (thick red line). The dashed lines are the acoustic (black) and optical (red) spin wave dispersions calculated using the fitting parameters. The grey area represents our energy/momentum resolution. (b) Experimental magnon dispersion in AF $Nd_{1.2}Ba_{1.8}Cu_3O_6$, underdoped $Nd_{1.2}Ba_{1.8}Cu_3O_7$, $YBa_2Cu_3O_{6.6}$, $YBa_2Cu_4O_8$ and $YBa_2Cu_3O_7$. Low-frequency INS data recorded from $\mathbf{Q}_{AF}$ for $YBa_2Cu_3O_{6.6}$ have been added. Lines are guides to the eye. (c) HWHM of magnetic excitations in $Nd_{1.2}Ba_{1.8}Cu_3O_7$, $YBa_2Cu_3O_{6.6}$, $YBa_2Cu_4O_8$ and $YBa_2Cu_3O_7$. (d) Integrated inelastic intensities.

The magnetic excitation energies of doped compounds at the Brillouin zone boundary are nearly identical to the ones found in $NdBCO_6$. This implies that the in-plane exchange constant $J_{//}$ is not as strongly renormalized with doping as previously suggested based on extrapolation of lower-energy INS data. Upon approaching the Γ point ($Q_{//} = 0$), we observe that the dispersion in the doped compounds is steeper than in $NdBCO_6$. Despite the fact that Γ and $\mathbf{Q}_{AF}$ are no longer equivalent in the absence of magnetic long-range order, the RIXS data obtained on $YBCO_{6.6}$ nicely extrapolate to the low-energy "hour glass" dispersion around $\mathbf{Q}_{AF}$ previously extracted from INS data on samples prepared in an identical manner. The intrinsic HWHM of ~ 200 meV of the inelastic signal extracted from our data (Fig. 3c) is much larger than the instrumental resolution and comparable to the magnon energies, indicating strong damping by Stoner excitations. The damping rate does not change substantially with $Q_{//}$ and with doping, and, remarkably, the integrated intensity of these excitations is conserved upon doping from the AF insulator to the slightly overdoped superconductor. We have thus demonstrated the existence of paramagnons, *i.e.* damped but well-defined, dispersive magnetic excitations, deep in the Stoner continuum of cuprates with doping levels beyond optimal doping. Their spectral weights are similar to those of spin waves in

the undoped, antiferromagnetically ordered parent material.

In order to obtain insight into the origin of this surprising observation, we have performed exact-diagonalization calculations of the $t-J$ Hamiltonian with $J/t = 0.3$ on finite-sized clusters.We used clusters with 18 and 20 spins arranged in various shapes to map the (H,K,0) reciprocal plane with sufficient momentum resolution and convoluted the resulting spectra by a Gaussian function with HWHM $0.1t$ in order to simulate the experimental resolution function. The calculated imaginary part of the spin susceptibility is shown in Fig. 3a for different hole concentrations. In the undoped case, one can distinguish two features: an intense peak corresponding to the single-magnon excitation, and a weaker feature at higher energy corresponding to higher-order processes. The single-magnon peak clearly disperses, although its energy is slightly above the value expected from linear spin-wave theory (dotted lines), due to the finite size of the cluster. In the inset of Fig. 4a, we present the energy-integrated magnetic intensity in the (H,K,0) reciprocal plane. As expected, the intensity for in the undoped situation is strongly peaked at $\mathbf{Q}_{AF}$, and rather uniformly distributed in the rest of the plane. As holes are added to the clusters, the magnetic spectral weight strongly decreases only around $\mathbf{Q}_{AF}$, but remains essentially constant everywhere else. This can also be seen in Fig. 4b, where the imaginary part of the energy-integrated spin susceptibility is plotted as a function of doping. The experimental and numerical data are thus in excellent agreement.

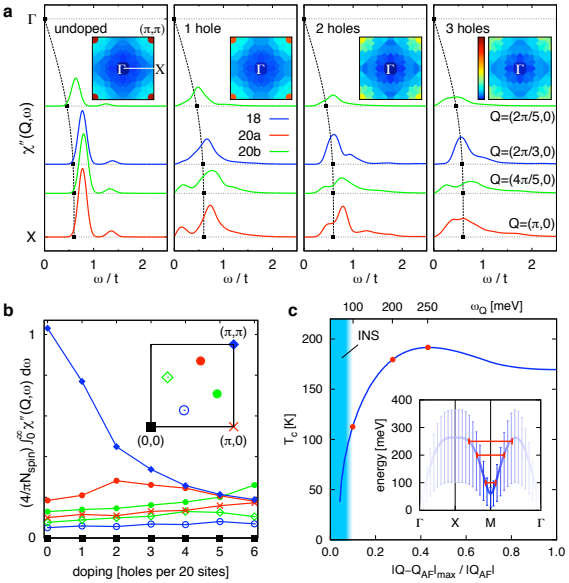

Figure 3: a) Imaginary part of the spin susceptibility resulting from exact diagonalization of the $t-J$ model on small clusters. The spectra are broadened using a Gaussian with HWHM$= 0.1t$. Dashed lines correspond to the linear spin wave dispersion. Insets: Brillouin-zone-maps of energy-integrated χ'' with a common color scale. b) Energy-integrated χ'' of the 20-site cluster, normalized to the number of electrons on the cluster, as a function of doping. The seven accessible non-equivalent $\mathbf{q}$-vectors for this cluster are shown in the inset. c) Superconducting transition temperature resulting from the Eliashberg calculation for the experimentally determined spin excitation spectrum of $YBCO_7$ displayed in the inset. Vertical bars account for the experimentally determined linewidths. The red marks indicate the influence of momentum-space cutoffs limiting the maximum distance from $\mathbf{Q}_{AF}$ of the $\mathbf{Q}$-vectors for which $\chi(\boldsymbol{Q},\omega)$ is included in the calculation.

Armed with essentially complete knowledge of the spin fluctuation spectrum, we have estimated the superconducting transition temperature T_c generated by a Cooper pairing mechanism in which the experimentally detected spin fluctuations play the role of bosonic glue. To this end, we have self-consistently solved the Eliashberg equations using the vertex function of the $t-J$ model and the experimental spin fluctuation spectrum of $YBCO_7$ (inset in Fig. 3c), without adjustable parameters. Figure 4c shows the outcome of the calculation. The resulting T_c of 170 K is similar to the maximum T_c observed in the cuprates and to another recent estimate based on the comparison of INS and photoemission data on underdoped $YBCO_{6+x}$ (ref. 1). The agreement with the experimentally observed T_c of $YBCO_7$ is satisfactory in view of the simplifying assumptions in the calculation, and in view of a similar level of quantitative agreement reported for Eliashberg calculations of conventional low-T_c superconductors. In order to resolve the relative contribution of the strongly doping dependent region around $\mathbf{Q}_{AF}$ and the high-energy part of the spin susceptibility revealed by RIXS to the pairing strength, we have introduced momentum cutoffs around $\mathbf{Q}_{AF}$ in the calculation (Fig. 3c). Clearly, both low- and high-energy spin fluctuations contribute substantially to the pairing. In underdoped cuprates, vertex corrections are expected to become essential, reducing the T_c values calculated here. These corrections suppress coupling to magnons in the vicinity of $\mathbf{Q}_{AF}$, leaving the contribution of the higher-energy excitations as a vital source of pairing.

References:

[1] *Dahm, T. et al.*, Nature Physics, **5**, 217 (2009).

[2] *Braicovich, L. et al.*, Physical Review Letters, **104**, 077002 (2010).

In collaboration with:

G. Ghiringhelli, M. Moretti Sala, M. Minola, L. Braicovich (Politecnico di Milano, Milano)

M. Salluzzo, G. M. De Luca (CNR-SPIN, Napoli)

T. Schmitt, C. Monney, K. J. Zhou (Paul Scherrer Institut, Villigen, Switzerland)